JOURNAL OF VIROLOGY, May 2000, p. 4319–4326 Vol. 74, No. 9
0022-538X/00/$04.00+0


# Infectious Bronchitis Virus E Protein Is Targeted to the Golgi Complex and Directs Release of Virus-Like Particles

EMILY CORSE AND CAROLYN E. MACHAMER*

*Department of Cell Biology and Anatomy, The Johns Hopkins University School of Medicine, Baltimore, Maryland 21205*

Received 14 December 1999/Accepted 3 February 2000

**The coronavirus E protein is a poorly characterized small envelope protein present in low levels in virions. We are interested in the role of E in the intracellular targeting of infectious bronchitis virus (IBV) membrane proteins. We generated a cDNA clone of IBV E and antibodies to the E protein to study its cell biological properties in the absence of virus infection. We show that IBV E is an integral membrane protein when expressed in cells from cDNA. Epitope-specific antibodies revealed that the C terminus of IBV E is cytoplasmic and the N terminus is translocated. The short luminal N terminus of IBV E contains a consensus site for N-linked glycosylation, but the site is not used. When expressed using recombinant vaccinia virus, the IBV E protein is released from cells at low levels in sedimentable particles that have a density similar to that of coronavirus virions. The IBV M protein is incorporated into these particles when present. Indirect immunofluorescence microscopy showed that E is localized to the Golgi complex in cells transiently expressing IBV E. When coexpressed with IBV M, both from cDNA and in IBV infection, the two proteins are colocalized in Golgi membranes, near the coronavirus budding site. Thus, even though IBV E is present at low levels in virions, it is apparently expressed at high levels in infected cells near the site of virus assembly.**

Coronaviruses are enveloped positive-strand RNA viruses. In contrast to many of the well-studied enveloped viruses that bud from the plasma membrane of cells, coronaviruses acquire their membrane envelope by budding into the lumen of Golgi and pre-Golgi compartments. After budding, virions are thought to move in vesicles through the secretory pathway and to exit the cell when these vesicles fuse with the plasma membrane (11, 34). The specific compartment into which coronaviruses bud is the *cis*-Golgi network (CGN), also known as the endoplasmic reticulum-Golgi intermediate compartment (15). The mechanism of budding-site selection is unclear. Just as enveloped viruses that bud from the plasma membrane must direct the accumulation of their envelope proteins at the cell surface, coronaviruses must localize their envelope proteins to the membranes of the *cis*-Golgi network. The possible role of the targeting of the individual membrane proteins in coronavirus budding-site selection has been studied by expressing them from cDNA in cultured cells.

The coronavirus avian infectious bronchitis virus (IBV) has three known membrane proteins. The spike (S) protein is a large glycoprotein involved in target cell recognition and fusion (6). When IBV S is expressed alone, it is transported to the plasma membrane (36), and so it is unlikely that S alone is responsible for determining the site of virus budding. The matrix (M) protein is a glycoprotein with three transmembrane domains; its large C terminus is thought to bind to the nucleocapsid during budding (17, 32). IBV M is found in the *cis*-Golgi network and *cis*-Golgi complex when expressed alone (23), and thus it reaches a slightly later compartment than the IBV budding site (13). The envelope (E) protein, due to its small size and low level in virions, has not been well characterized. However, it is associated with the virion envelope (20, 30).

Evidence from studies of other coronaviruses suggests the coronavirus E protein is likely to play an important role in virus assembly. When the E and M proteins from either mouse hepatitis virus (MHV) or transmissible gastroenteritis virus (TGEV) are expressed together in cells from cDNA, virus-like particles (VLPs), roughly the same size and shape as virions, are released from the cells (3, 25, 37). These results have been suggested to indicate that coronavirus E and M proteins constitute the minimal assembly machinery. However, expression of the MHV E protein alone was recently found to be sufficient for VLP production (25). The envelope protein S is incorporated into VLPs when present but is not necessary for particle formation (37). "Infectious" MHV VLPs containing S and the viral nucleocapsid protein (N) require E and M to transfer a synthetic viral RNA to new cells (4). Studies of MHV defective interfering (DI) RNAs, which are incomplete genomic RNAs, have shown that a naturally occurring DI RNA, containing only the coding sequence for the viral polymerase and nucleocapsid proteins, can be complemented with a synthetic DI RNA encoding the E and M proteins to generate particles that are released from cells (12). Finally, viruses with mutations in MHV E, generated by RNA recombination techniques, have aberrantly shaped virions (7).

We have studied the cell biological properties of the IBV E protein as a prerequisite to investigating its role in virus assembly. We show that IBV E is integrally associated with cellular membranes, with its C terminus in the cytoplasm. Expression of IBV E from cDNA resulted in its release from cells in sedimentable particles, which incorporated IBV M protein if present. Indirect immunofluorescence and confocal microscopy of cells expressing IBV E showed that it is targeted to the Golgi complex. When IBV E and M proteins were coexpressed, either by infection with recombinant vaccinia viruses or by infection with IBV, the two proteins colocalized in the Golgi complex near the virion budding site.

* Corresponding author. Mailing address: Department of Cell Biology and Anatomy, The Johns Hopkins University School of Medicine, 725 N. Wolfe St., Baltimore, MD 21205. Phone: (410) 955-1809. Fax: (410) 955-4129. E-mail: machamer@jhmi.edu.

## MATERIALS AND METHODS

**Cells and viruses.** BHK-21 and HeLa cells were maintained in Dulbecco's modified Eagle's medium (DMEM) containing 5% fetal calf serum (FCS) and

antibiotics, and Vero cells were maintained in DMEM with 10% FCS and antibiotics. 143B cells were grown in DMEM with 10% FCS, antibiotics, and 25 μg of 5-bromodeoxyuridine per ml. The adaptation of IBV (Beaudette strain) to Vero cells has been described previously (22). The recombinant vaccinia viruses encoding phage T7 RNA polymerase (vTF7-3 [8]), and IBV M (vvIBVM [22]) have been previously described. The recombinant vaccinia virus encoding IBV E (vvIBVE) was made by established methods, by subcloning E from pBS/IBVE (see below) into pSC11MCS1 (10), which contains the early vaccinia virus promoter p7.5, using the *Apa*II and *Sac*I retriction sites. The resulting plasmid was transfected into HeLa cells infected with wild-type vaccinia virus (WR strain) and allowed to recombine with the viral thymidine kinase gene. Recombinant viruses were selected in 143B cells, which are null for thymidine kinase, and plaque purified. Large-scale preparations of recombinant viruses were grown and subjected to titer determination as described previously (39).

**Expression vectors.** The coding region of IBV E was subcloned by PCR from p57-6 (22). The 5′ primer was designed to contain an *Eco*RI site and the first three codons of IBV E, which are not present in p57-6, and the 3′ primer contained a *Bam*HI site. IBV E was cloned into pBluescript SK (Stratagene, La Jolla, Calif.) behind the T7 promoter, using *Eco*RI and *Bam*HI to generate pBS/IBV E, and the sequence of the IBV E open reading frame was confirmed by dideoxy sequencing. The pBS/IBV E plasmid was used to express IBV E in vTF7-3-infected cells. IBV M was expressed in vTF7-3-infected cells from pAR/IBVM, which contains a T7 promoter and was generated by subcloning the coding sequence for M from pSV/IBVE1 (22) into pAR2529-X at the *Xho*I site. Gm1, a Golgi-retained chimeric protein consisting of the ectodomain and cytoplasmic tail of vesicular stomatitis virus (VSV) G protein and the first transmembrane domain of IBV M, was expressed in vTF7-3-infected cells behind the T7 promoter as described (33).

**Antibodies.** Synthetic peptides corresponding to the 14 amino-terminal and 14 carboxy-terminal amino acids of IBV E (each with an added cysteine residue) were synthesized, purified, and coupled to keyhole limpet hemocyanin by Boston Biomolecules, Inc. (Boston, Mass.). Polyclonal antibodies recognizing the amino terminus and carboxy terminus of IBV E were made in rabbits by immunizing with these peptides. The rat polyclonal anti-E antibody was made against the carboxy-terminal E peptide. The rabbit anti-E antibodies were affinity purified for use in indirect immunofluorescence by using the Reduce-Imm reducing kit and the Sulfolink kit (Pierce, Rockford, Ill.) as specified by the manufacturer. The affinity-purified polyclonal anti-IBV M antibody used in immunofluorescence has been described previously (22). The polyclonal anti-IBV M antibody used in immunoprecipitations was generated in rabbits against a peptide corresponding to the carboxy-terminal 14 amino acids as described previously (22). The polyclonal antibody against whole IBV virions was made by immunizing rabbits with purified UV-inactivated IBV virions. Virions were prepared as described previously (31), except that the virus was grown in Vero cells. Antibodies to Gm1 were the mouse monoclonal antibody I1, which recognizes the luminal domain of VSV G (18), and a polyclonal antibody, recognizing the cytoplasmic tail, raised in rabbits to the C-terminal 14 amino acids of VSV G protein. The mouse monoclonal antibodies to GM130 and syntaxin 6 were purchased from Transduction Laboratories, (Lexington, Ky.), and the mouse monoclonal anti-mannosidase II antibody was purchased from Berkeley Antibody Co. (Richmond, Calif.). Texas Red-conjugated goat anti-rabbit, anti-mouse, and anti-rat immunoglobulin G (IgG) and fluorescein-conjugated goat anti-rabbit and anti-mouse IgG were from Jackson ImmunoResearch Laboratories, Inc. (West Grove, Pa.).

**Immunofluorescence and confocal microscopy.** For localization studies of IBV E and IBV M in recombinant vaccinia virus-infected cells, BHK-21 cells were plated on coverslips in 35-mm dishes 1 day before infection. vvIBVE or vvIBVE plus vvIBVM were adsorbed at a multiplicity of infection of 5 for each virus in 0.5 ml of serum-free DMEM for 30 min at 37°C. At 6 h postinfection, the cells were fixed in 3% paraformaldehyde in phosphate-buffered saline for 20 min at room temperature, permeabilized with 0.5% Triton X-100, and stained as previously described (33), using affinity-purified anti-IBV E raised to the C terminus. For selective permeabilization of the plasma membrane with digitonin, BHK-21 cells were infected with vTF7-3 (adsorption as above except that Opti-MEM [Life Technologies, Rockville, Md.] was used) and then transfected with 5 μg of a plasmid encoding Gm1 using 10 μl of Lipofectin (Life Technologies), as specified by the manufacturer, or infected with vvIBVE as described above. At 6 h postinfection, the cells were transferred to ice, rinsed in KHM (110 mM potassium acetate, 20 mM HEPES [pH 7.2], 2 mM magnesium acetate), and permeabilized for 5 min on ice with 25 μg of digitonin per ml in KHM as described previously (29). Fixation and staining were as described above, with no subsequent permeabilization step. Images were collected with a Pascal 510 confocal laser-scanning microscope (Zeiss) or a Noran OZ confocal laser-scanning microscope using Intervision software on a Silicon Graphics Indy R5000 platform. All images shown are 0.5-μm optical slices in the *z* axis near the center of the cell.

**Metabolic labeling, alkaline carbonate extraction, glycosidase digestion, and immunoprecipitation.** Cells infected with vTF7-3 and transfected with either pBS/IBVE, pAR/IBVM, pAR/VSVG, or pAR/VSVG$_{soluble}$ as described above were radiolabeled from 3.5 to 4.5 h postinfection with 50 μCi of $^{35}$S-Promix (Amersham Pharmacia Biotech, Inc., Piscataway, N.J.) in methionine- and cysteine-free medium. For alkaline carbonate extraction, cells were homogenized in 15 mM NaCl–10 mM Tris-HCl (pH 7.4)–1 mM $MgCl_2$–8% sucrose by 60 strokes in a tight-fitting Dounce homogenizer. Nuclei were pelleted by centrifugation, and the supernatant was adjusted to 0.1 M $Na_2CO_3$ (pH 11.5) and incubated 10 min on ice. A control sample was incubated in 0.1 M NaCl under the same conditions. Membranes were pelleted in a Beckman TLA100 rotor at 132,000 × *g* for 1 h. The supernatant was adjusted to pH 7, 1% Triton X-100, and 0.2% sodium dodecyl sulfate (SDS), and the pellet was resuspended in detergent solution (62.5 mM EDTA, 50 mM Tris [pH 8], 0.4% deoxycholate, 1.0% Nonidet P-40). The supernatant and pellet were immunoprecipitated with the appropriate antibodies as previously described (22). The immunoprecipitates were analyzed by polyacrylamide gel electrophoresis (PAGE) in the presence of SDS and visualized by fluorography. For *N*-glycanase digestion, cells were lysed in detergent solution with protease inhibitors and immunoprecipitated with the appropriate antibodies as described previously (22). The immunoprecipitates were treated with *N*-glycanase as described previously (23), separated by SDS-PAGE on a 15% polyacrylamide gel, and visualized by fluorography.

**Western blotting.** Vero cells infected with IBV were lysed in 2× SDS sample buffer–5% β-mercaptoethanol, and the lysates were subjected to SDS-PAGE. Proteins were transferred to nitrocellulose, and the membrane was blocked with 5% nonfat milk in 10 mM Tris (pH 7.4)–150 mM NaCl–0.05% Tween 20 for 1 h at room temperature. Incubation with primary antibodies was carried out overnight at 4°C in the same buffer. The membrane was washed extensively before being incubated with peroxidase-conjugated sheep anti-rabbit IgG for 1 h at room temperature in the same buffer, followed by extensive washing. Bound antibody was detected with SuperSignal West Pico chemiluminescent substrate (Pierce).

**Detection and equilibrium centrifugation of VLPs.** Dishes (diameter, 10 cm) of BHK-21 cells were infected with vvIBVE and or vvIBV E and vvIBVM at a multiplicity of infection of 10 for each virus. At 3.5 h postinfection, the cells were radiolabeled with 500 μCi of $^{35}$S-Promix (Amersham) in methionine- and cysteine-free medium for 1 h and chased for 3 h with medium containing excess unlabeled cysteine and methionine. Medium was collected and cleared by centrifugation at 1,000 × *g* for 10 min. Concentrated detergent solution was added, and the samples were immunoprecipitated with anti-E and anti-M antibodies. The immunoprecipitates were separated by SDS-PAGE on 15% polyacrylamide gels. Each lane contained the immunoprecipitate from two 10-cm dishes. For equilibrium density centrifugation, chase medium was collected, cleared by centrifugation at 1,000 × *g* for 10 min, and concentrated by pelleting onto 55% sucrose in TNE (50 mM Tris [pH 7.4], 100 mM NaCl, 1 mM EDTA) by centrifugation at 130,000 × *g* for 2 h in a Beckman SW41 rotor. The medium/sucrose interface was collected, diluted in TNE, and loaded onto a continuous gradient of 20 to 55% sucrose in TNE. The gradients were centrifuged at 130,000 × *g* for 18 h, and 1-ml fractions were collected from the top. Each fraction was immunoprecipitated with the appropriate antibodies, and the immunoprecipitates were electrophoresed and visualized by fluorography. Each gradient was loaded with the supernatant from four 10-cm dishes of vaccinia virus-infected cells.

## RESULTS

**Detection of IBV E in transfected and IBV-infected cells.** For expression of IBV E in the absence of the other viral proteins, a recombinant vaccinia virus encoding the protein was generated. Antipeptide polyclonal antibodies were made against the amino and carboxy termini of IBV E in rabbits and toward the carboxy terminus in rats. BHK-21 cells expressing IBV E by infection with vvIBVE were radiolabeled and immunoprecipitated with each of these antibodies and the corresponding preimmune sera. Upon electrophoresis of the immunoprecipitates, a specific band of 12 kDa corresponding to the E protein was visualized in each of the samples immunoprecipitated with immune sera but was not seen in samples immunoprecipitated with preimmune sera (Fig. 1a). Figure 1b shows Western blots of IBV-infected Vero cell lysates collected at various times postinfection. The blot in the top panel of Fig. 1b was probed with antibodies to IBV E and IBV M and shows that these two proteins were detected by 36 and 24 h postinfection, respectively. The bottom panel of Fig. 1b demonstrates that the IBV E protein was not detected when the same lysates were probed with antibody generated against whole virions. This result was not surprising, given the low level of IBV E present in virions (20).

**IBV E is an integral membrane protein.** IBV E was shown to be associated with purified virions (20), and its sequence predicts a single hydrophobic domain. Microsomal membranes from radiolabeled BHK-21 cells expressing IBV E were sub-

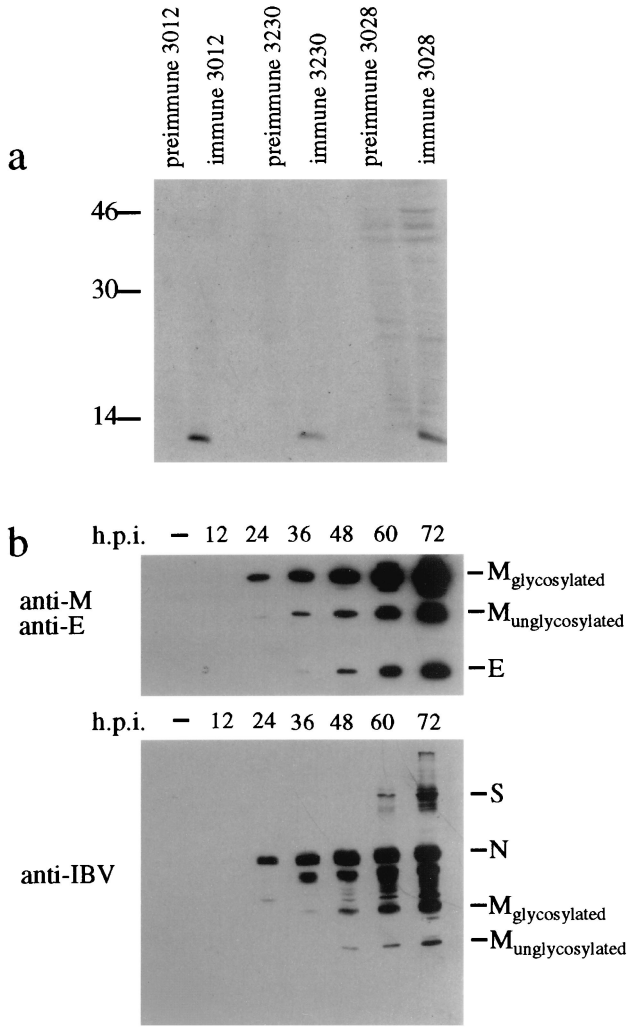


FIG. 1. Antibodies recognizing the IBV E protein are specific. (a) BHK-21 cells infected with vvIBVE were radiolabeled from 3.5 to 4.5 h postinfection and lysed in detergent solution. The lysates were immunoprecipitated with polyclonal peptide antibodies to IBV E and the corresponding preimmune sera. The immunoprecipitates were analyzed by SDS-PAGE on a 15% polyacrylamide gel and visualized by fluorography. 3012 is the rabbit anti-C-terminal peptide antibody, 3230 is the rat anti-C-terminal peptide antibody, and 3028 is the rabbit anti-N-terminal peptide antibody. (b) Vero cells infected with IBV were harvested after infection for the times shown in SDS sample buffer. The samples were subjected to SDS-PAGE and Western blotting with anti-E and anti-M antibodies (top) or anti-IBV antibodies (bottom). The lanes labeled – contain lysate from mock-infected cells. h.p.i., hours postinfection.

jected to alkaline carbonate extraction to assess whether IBV E was an integral membrane protein. After extraction for 10 min at 0°C with 0.1 M NaCl (control) or 0.1 M $Na_2CO_3$ (pH 11.5), samples were centrifuged and the membrane pellets and supernatants were subjected to immunoprecipitation with anti-E antibodies. The association of IBV E with the pelleted membranes in the presence of 0.1 M $Na_2CO_3$ indicates that it is an integral membrane protein (Fig. 2). Controls were performed using VSV G protein, a known integral membrane protein, and VSV $G_{soluble}$, a secreted form of G which lacks the transmembrane domain (data not shown). VSV G was associated with the pelleted membranes in the presence of both 0.1 M NaCl and 0.1 M $Na_2CO_3$, which is consistent with its integral membrane association. VSV $G_{soluble}$ pelleted with membranes after 0.1 M NaCl treatment but was extracted from

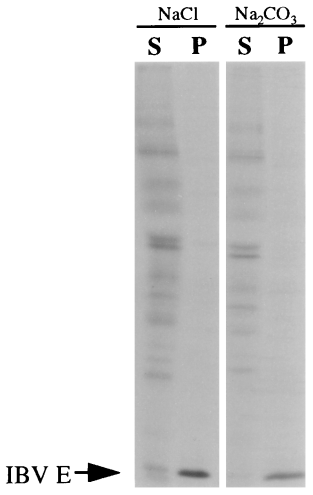


FIG. 2. IBV E is an integral membrane protein. BHK-21 cells infected with vvIBVE were radiolabeled from 3.5 to 4.5 h postinfection, and microsomes were prepared from homogenized cells. The microsomes were extracted with either 0.1 M NaCl (left) or 0.1 M $Na_2CO_3$, (pH 11.5) (right), and the membranes were pelleted. Pellets (P) and supernatants (S) were immunoprecipitated with anti-IBV E in the presence of detergent, and the immunoprecipitates were analyzed by SDS-PAGE on a 15% polyacrylamide gel and visualized by fluorography.

membranes with 0.1 M $Na_2CO_3$, as expected for a nonintegral, secreted protein.

**Membrane topology of IBV E.** To determine the orientation of IBV E in membranes, we used antibodies specific for the N and C termini of the protein. Preliminary indirect-immunofluorescence microscopy suggested that IBV E was localized to an intracellular juxtanuclear compartment when expressed alone from cDNA (see Fig. 6). BHK-21 cells transiently expressing the E protein were permeabilized with digitonin, which at low concentrations selectively permeabilizes the plasma membrane but leaves intracellular membranes intact (29). To confirm that intracellular membranes were indeed not permeabilized when the cells were treated with digitonin, BHK-21 cells transiently expressing the Golgi-resident Gm1 protein (33) were stained with antibodies specific either to the luminal head domain (Fig. 3b and f) or to the cytoplasmic tail domain (Fig. 3a and e). The cytoplasmic tail epitope should always be accessible to antibody when the plasma membrane is permeabilized, while the luminal epitope should be accessible only when Golgi membranes are also permeabilized. As expected, the cytoplasmic tail domain of Gm1 was accessible to antibody when the cells were permeabilized with either digitonin (Fig. 3e) or Triton X-100 (Fig. 3a), while the luminal head domain was not accessible to antibody when cells were permeabilized with digitonin (Fig. 3f), consistent with an unpermeabilized Golgi apparatus. The IBV E protein was accessible to C-terminus-specific antibodies in the presence of either digitonin (Fig. 3g) or Triton X-100 (Fig. 3c) but was accessible to N-terminus-specific antibodies only in the presence of Triton X-100 (Fig. 3d). These results are consistent with IBV E possessing a luminal N terminus, a cytoplasmic C terminus, and a single transmembrane domain.

**Posttranslational modifications of IBV E.** IBV E contains a consensus site for N-linked glycosylation very near its N terminus. Given that the N terminus is luminal (Fig. 3) and given the utility of glycosylation in studying trafficking of proteins, we performed *N*-glycanase digestion to determine if the site is used. BHK-21 cells transiently expressing the IBV E protein were radiolabeled and immunoprecipitated with anti-E anti-

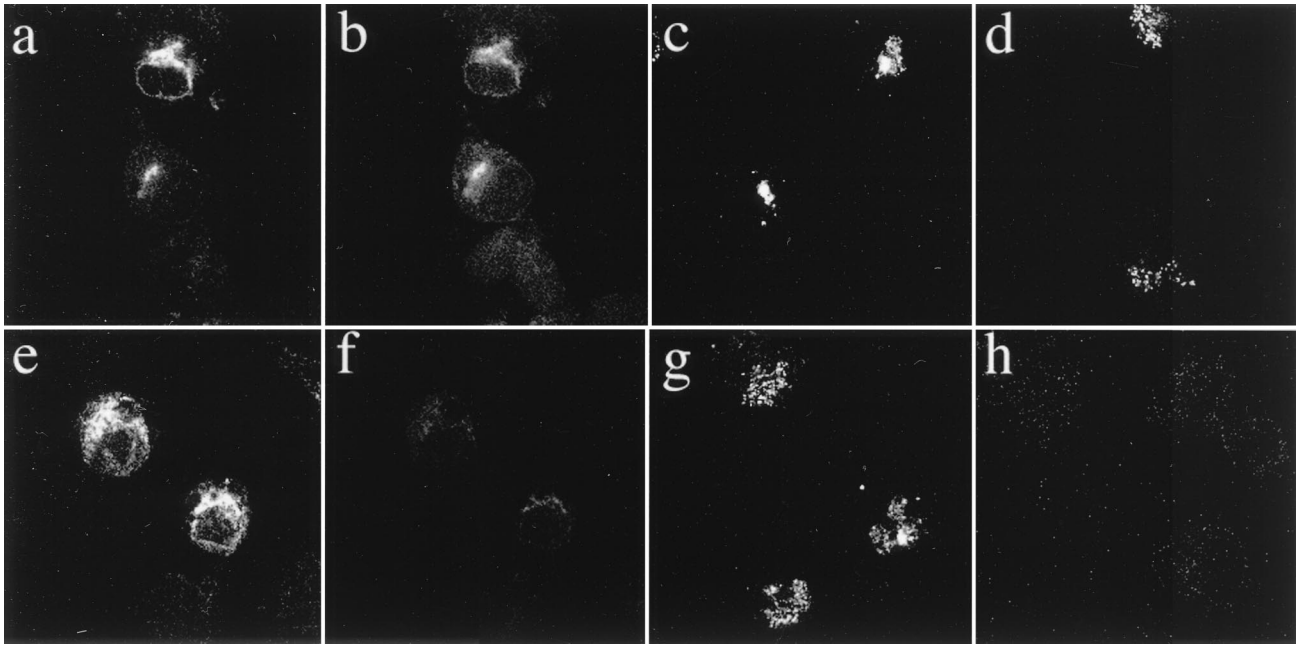


FIG. 3. The C terminus of IBV E is cytoplasmic. BHK-21 cells were infected with vTF7-3 and transfected with a plasmid encoding the Golgi resident protein Gm1 (a, b, e, and f) or infected with vvIBV E (c, d, g, and h) as described in Materials and Methods. At 6 h postinfection, cells were either permeabilized with digitonin (e to h) and fixed for immunofluorescence or fixed and permeabilized with Triton X-100 prior to staining (a to d). The cells were stained with antibodies to the cytoplasmic tail of Gm1 (a and e), the luminal head of Gm1 (b and f), the C terminus of IBV E (c and g), or the N terminus of IBV E (d and h). Secondary antibodies were fluorescein-conjugated goat anti-mouse IgG (b and f) and Texas red-conjugated goat anti-rabbit IgG (all other panels).

body. The immunoprecipitates were digested with *N*-glycanase. The results, shown in Fig. 4, indicate that IBV E does not undergo N-linked glycosylation, since its electrophoretic mobility does not change after treatment with *N*-glycanase. As a positive control for *N*-glycanase digestion, IBV M, which is known to have N-linked sugars (31), was also treated with *N*-glycanase and shown to increase in mobility under these conditions (Fig. 4).

IBV E, like other coronavirus E proteins, contains cysteine residues adjacent to its transmembrane domain, and there is evidence that MHV E is posttranslationally acylated (40). However, we were unable to detect incorporation of [$^3$H]palmitate into the IBV E protein in BHK-21 cells (data not shown).

**Release of VLPs from cells expressing IBV E and M.** We determined if VLPs could be generated by expression of IBV E and M, as reported for other coronaviruses (3, 25, 37). IBV E and M were expressed using the recombinant vaccinia viruses vvIBVE and vvIBVM (22). Cells were radiolabeled from 3.5 to 4.5 h postinfection and chased for 3 h. Supernatants were collected, cleared of debris, and immunoprecipitated with antibodies to E and M (Fig. 5a). IBV E was released into the supernatant regardless of whether IBV M was present in transfected cells. However, IBV M was not released into the supernatant unless IBV E was present. These results suggest that E is required for the release of these proteins from cells, because M was not released when expressed alone.

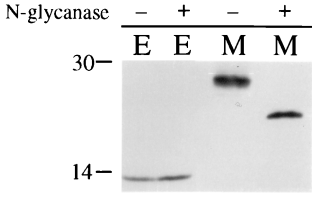


FIG. 4. The N-terminal N-linked glycosylation site of IBV E is not used. BHK-21 cells infected with vTF7-3 were transfected with plasmids encoding IBV E or IBV M, radiolabeled from 3.5 to 4.5 h postinfection and lysed in detergent solution. The lysates were immunoprecipitated with appropriate antibodies to E or M. The immunoprecipitates were mock treated (−) or treated with *N*-glycanase (+), analyzed by SDS-PAGE on a 15% polyacrylamide gel, and visualized by fluorography.

To determine whether the proteins are released in sedimentable particles, as shown for other coronaviruses, the supernatants from cells expressing E or E and M together were loaded onto 20 to 55% sucrose gradients and centrifuged to equilibrium. Fractions were collected and immunoprecipitated with appropriate antibodies. The immunoprecipitates were electrophoresed and visualized by fluorography, and the results are shown in Fig. 5b (E and M) and c (E alone). The presence of E and M proteins in fractions 4, 5, and 6 (Fig. 5b) shows that the proteins released into the supernatant are present in sedimentable particles. Fraction 5, which contained the majority of the M protein, had a density of 1.11 g/cm$^3$. The E protein was also released from cells in sedimentable particles when expressed alone, as shown in Fig. 5c. The peak density for the E protein, both when coexpressed with M and when expressed alone, occurred between fractions 5 and 6 and was measured to be 1.14 g/cm$^3$. These results differ from those reported for MHV E and M proteins, where particles containing both proteins were shown to be denser than those containing MHV E alone (25). The difference might be explained by our observation that the level of IBV E protein released from cells expressing E alone was consistently greater than that of E released from cells expressing both E and M proteins (Fig. 5a). We noted that the release of both types of particles occurred at extremely low efficiency, since the supernatants contained less than 0.01% of cellular E or M proteins.

We also attempted to assess IBV E and IBV M interactions

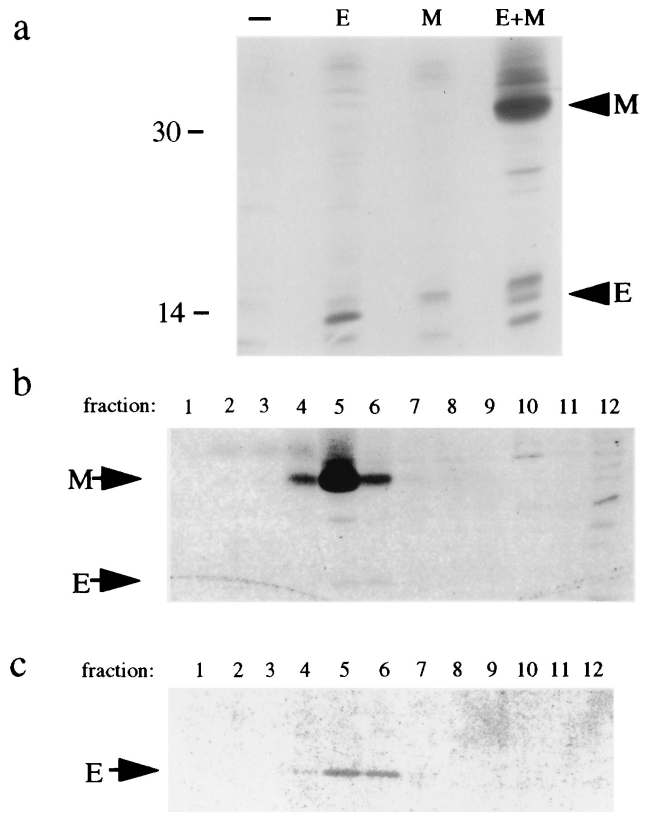


FIG. 5. IBV E is released from transfected cells in VLPs that incorporate IBV M if present. (a) BHK-21 cells were mock infected (−), infected with vvIBVE (E), vvIBVM (M), or vvIBVE plus vvIBVM (E+M), radiolabeled from 3.5 to 4.5 h postinfection, and chased for 3 h. Medium was collected, cleared of debris, and immunoprecipitated with anti-E and anti-M antibodies. The immunoprecipitates were analyzed by SDS-PAGE and visualized by fluorography. (b) BHK-21 cells coinfected with vvIBVE and vvIBVM were radiolabeled from 3.5 to 4.5 h postinfection and chased for 3 h. Concentrated supernatants were loaded onto a continuous 20 to 55% sucrose gradient and centrifuged to equilibrium. Fractions were collected and immunoprecipitated with anti-E and anti-M antibodies. The immunoprecipitates were separated by SDS-PAGE and visualized by fluorography. Fraction 1 corresponds to the top of the gradient, and fraction 12 corresponds to the bottom of the gradient. (c) BHK-21 cells were infected with vvIBVE only and treated exactly as described for panel b.

by coimmunoprecipitation from recombinant vaccinia virus-infected cells, but we found no evidence for stable association between the two proteins (data not shown). Also, the rate of IBV M trafficking, measured by monitoring the processing of its N-linked oligosaccharides at different times after synthesis, was unchanged in cells coexpressing IBV E (data not shown). Thus, it appears that IBV E and IBV M do not interact strongly in transfected cells or in detergent lysates.

**IBV E is targeted to the Golgi complex.** To establish the intracellular localization of IBV E, BHK-21 cells infected with vvIBVE were analyzed by indirect immunofluorescence using confocal microscopy. A juxtanuclear staining pattern was observed, which was compared with the localizations of three endogenous Golgi marker proteins (Fig. 6). The endogenous Golgi proteins that were analyzed were GM130, a *cis*-Golgi resident (26), mannosidase II, a Golgi stack marker (35), and syntaxin 6, a *trans*-Golgi network and endosomal resident (5). The red images (Fig. 6a, e, and i) show the intracellular distribution of the IBV E protein, and the green images (Fig. 6b, f, and j) show that of each marker protein. The third image in every row (Fig. 6c, g, and k) corresponds to the overlay of red and green images; yellow represents regions of overlap between the red- and green-staining patterns. The staining pattern of IBV E was most similar to that of mannosidase II, whereas there was somewhat less overlap with either GM130 or syntaxin 6. These results demonstrate that IBV E is targeted to Golgi membranes in the absence of the other IBV proteins and that it reaches the Golgi stacks, where it appears to accumulate. No plasma membrane staining was observed in IBV E-expressing cells.

**Colocalization of IBV E and IBV M in vaccinia virus- and IBV-infected cells.** We also investigated the distribution of IBV E in cells coexpressing IBV M. Figure 7a to d shows the results of a double labeling experiment in which BHK-21 cells coinfected with vvIBVE and vvIBVM were stained with antibodies to E and M. Confocal microscopy indicated that the distribution of the proteins completely overlapped (Fig. 7c). IBV E and M also colocalized in cells infected with IBV at 6 h postinfection (Fig. 7e to h). In IBV-infected cells, there was some additional reticular staining for IBV M, which probably corresponds to the endoplasmic reticulum (Fig. 7f). Even so, there was nearly complete overlap between the distribution of IBV E and M in IBV-infected cells. These results demonstrate that both IBV E and M proteins accumulate in infected cells near the site of virus budding.

## DISCUSSION

Coronaviruses are positive-strand RNA viruses that obtain their membrane envelope by budding into the CGN, also known as the endoplasmic reticulum-Golgi intermediate compartment (13, 15). The mechanism of budding-site selection is unclear, but the possible role of the targeting of individual coronavirus envelope proteins in this process has been examined by expressing them from cDNA. IBV M is localized to the *cis*-Golgi network and *cis*-Golgi complex when expressed alone (23) and thus reaches a slightly later compartment than that of the budding site. MHV M is found in the *trans*-Golgi network when expressed from cDNA (14), a compartment even more distant from the budding compartment. Thus, it is unlikely that the M protein is solely responsible for selection of the coronavirus budding site. The coronavirus S protein is found at the plasma membrane when expressed alone (36) and thus probably does not play a major role in selection of the CGN for budding. It seems likely that there is a general mechanism for the accumulation of coronavirus envelope proteins at the budding site so that efficient virus assembly can occur. The only other known coronavirus envelope protein, E, is incompletely characterized, and its subcellular localization has not been carefully studied. The work described here was carried out as a prerequisite to determining the role of IBV E in budding-site selection and virus assembly.

**Topology and intracellular localization of IBV E.** Using indirect-immunofluorescence microscopy in conjunction with the detergent digitonin, which selectively permeabilizes the plasma membrane of cells when used at low concentrations (29), and domain-specific antibodies generated against the IBV E protein, we showed that the carboxyl terminus of E is cytoplasmic. This topology is predicted from the positive-inside rule (38), and the E proteins of all coronaviruses contain a positively charged residue(s) on the C-terminal sides of their predicted transmembrane domains. This topology places IBV E in the type III class of integral membrane proteins (38), since it lacks a cleaved signal sequence. Given this topology of the IBV E protein, it was possible that the protein was N glycosylated at a consensus site near the N terminus. We showed that the glycosylation site is not used, probably because of its extreme

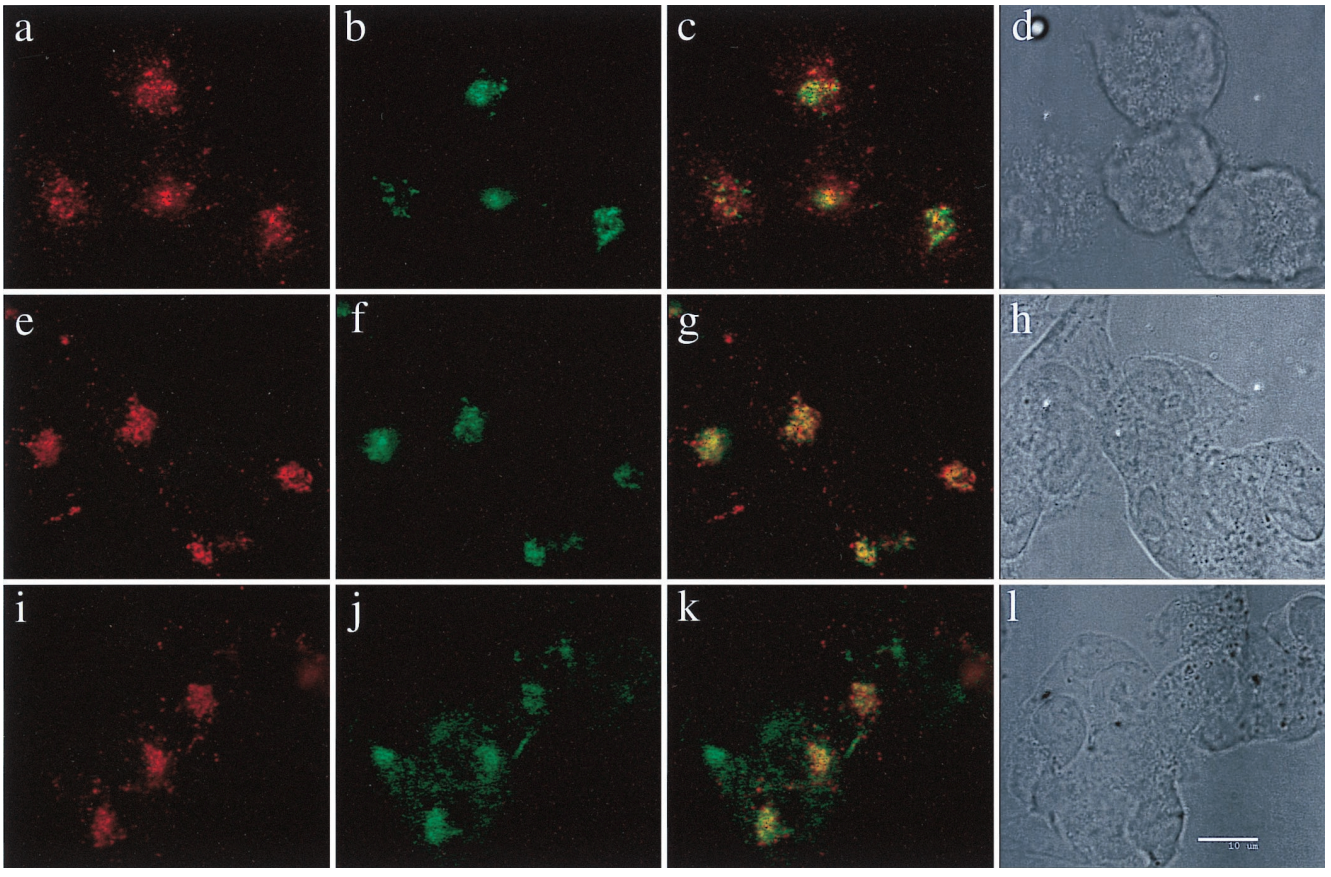


FIG. 6. The IBV E protein is localized to the Golgi complex. BHK-21 cells infected with vvIBVE were fixed for immunofluorescence at 6 h postinfection, permeabilized with Triton X-100, and double labeled with antibodies to IBV E and different endogenous Golgi resident proteins. (a to d) Cells were stained with rabbit anti-IBV E and mouse anti-GM130; (e to h) cells were stained with rabbit anti-IBV E and mouse anti-mannosidase II; (i to l) cells were stained with rabbit anti-IBV E and mouse anti-syntaxin 6. Secondary antibodies were Texas red-conjugated goat anti-rabbit IgG and fluorescein-conjugated goat anti-mouse IgG. In each row, the red image corresponds to IBV E staining and the green image corresponds to the appropriate Golgi marker. The third image in each row (c, g, and k) is a merged image, where yellow represents overlap between the red- and green-staining patterns. The fourth image in each row (d, h, and l) is a phase image of each field of labeled cells. Bar, 10 μm.

proximity to the membrane (27). The topology of IBV E determined here differs from that previously published for TGEV E (9). Godet et al. showed that the C terminus of cell surface TGEV E was extracellular because it was accessible to antibody in nonpermeabilized cells (9).

We showed by indirect immunofluorescence and confocal microscopy that the IBV E protein is localized to the Golgi complex in both transfected and IBV-infected cells. We did not detect IBV E at the cell surface, as described for bovine coronavirus E and TGEV E proteins (1, 9). When we compared the localization of IBV E to that of three marker proteins that reside in different regions of the Golgi complex, we found that the distribution of IBV E most closely overlapped that of mannosidase II, a Golgi stack marker. There was less, but significant, overlap with the *trans*-Golgi resident syntaxin 6 and the *cis*-Golgi protein GM130. The proximity of the subcellular distribution of the E protein to the coronavirus budding site is interesting in light of the hypothesis that E plays a role in directing the accumulation of coronavirus envelope proteins at the budding site. The IBV M protein is targeted to the *cis*-Golgi complex when it is expressed from cDNA, at least in part by information contained in its first transmembrane domain (23, 24, 33). Here we have shown that IBV encodes another envelope protein (E) that possesses Golgi targeting information. It will be interesting to dissect the targeting information in IBV E to determine whether E and M have a common mechanism for Golgi localization.

When the IBV E and M proteins were expressed together in cells, either by coinfection with recombinant vaccinia viruses or by IBV infection, they colocalized when analyzed by indirect immunofluorescence and confocal microscopy. This result is intriguing, since it may point to interactions between the E and M proteins that result in their localization in the same compartment. However, we were unable to demonstrate interactions between IBV E and M directly. We are interested in interactions that the E protein may have with the other IBV proteins and the possible role of these interactions in gathering the envelope proteins at the CGN for budding. We plan to further examine the targeting of the IBV E protein and the effect of its expression on the localization of IBV M at the ultrastructural level in order to address these questions.

**IBV VLPs are produced inefficiently.** When the IBV E and M proteins were transiently expressed in cells, they were released into the culture supernatants in sedimentable particles. We also observed that the IBV E protein was released in similar particles when expressed alone. These particles, when centrifuged to equilibrium on sucrose density gradients, had densities of 1.11 g/cm$^3$ (particles containing both E and M) and 1.14 g/cm$^3$ (particles containing E alone). The release of coronavirus E protein from cells in membranous particles has ob-

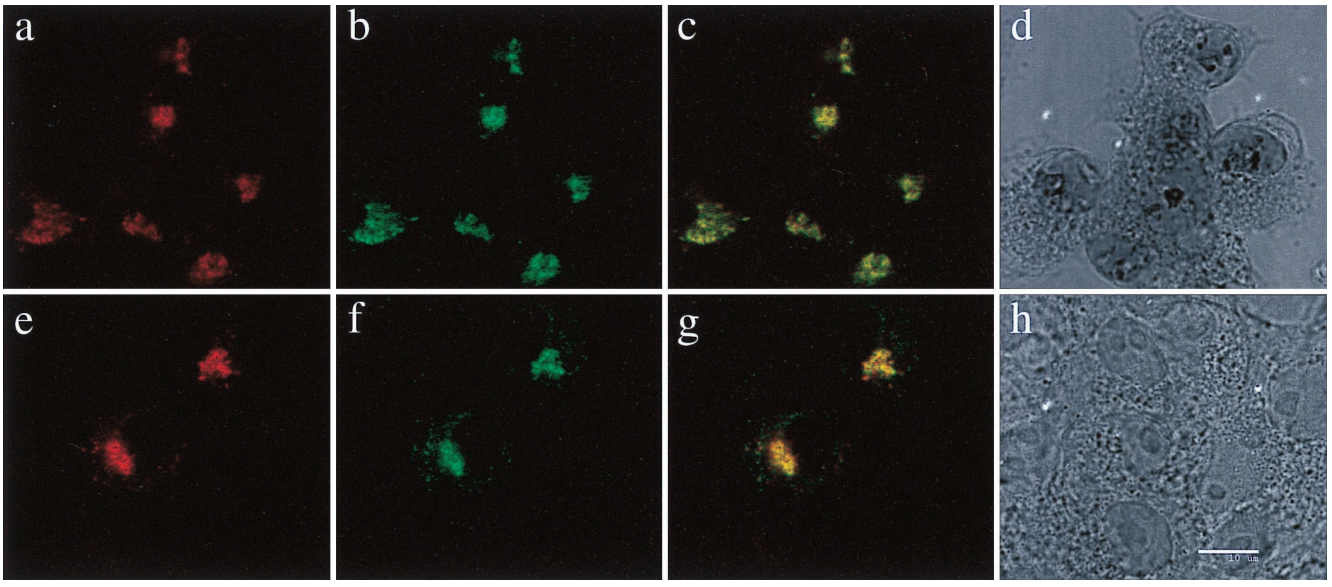


FIG. 7. IBV E and IBV M colocalize in transfected and IBV-infected cells. BHK-21 cells infected with vvIBVE and vvIBVM (a to d) or IBV-infected Vero cells (e to h) were fixed for immunofluorescence at 6 h postinfection and double labeled with rat anti-E antibody and rabbit anti-M antibody. Secondary antibodies were Texas red-conjugated goat anti-rat IgG and fluorescein-conjugated goat anti-rabbit IgG. The red images correspond to IBV E staining, and the green images correspond to IBV M staining. The third image in each row (c and g) is a merged image, where yellow represents overlap between the red- and green-staining patterns. The fourth image in each row (d and h) is a phase image of the field of labeled cells. Bar, 10 μm.

vious implications for the importance of the role of E in virus assembly. However, at least for IBV proteins in BHK-21 cells, particle release was extremely inefficient, since the amounts of E and M proteins released into the supernatant were less than 0.01% of the cellular E and M levels. Clearly, other IBV components must be required for efficient budding and/or release of virus from cells. The efficiency of VLP formation in cells expressing MHV and TGEV E and M proteins was not reported (3, 25, 37), and so it is not yet clear if the assembly mechanism of IBV differs from that of these other coronaviruses.

**Can the E protein drive IBV assembly?** It was proposed that coronavirus M and E proteins are the minimal assembly unit, since expression of these proteins resulted in their release in VLPs (37). This is unusual, since the assembly of many enveloped viruses is nucleocapsid dependent. Recently, it was shown that expression of MHV E alone induces VLPs (25), as we have shown here for IBV E. However, the efficiency of VLP release from cells expressing IBV E with or without M is extremely low. Therefore, it is not clear if IBV VLP production is relevant to virus assembly. IBV E is expressed from a tricistronic RNA (21), and the two open reading frames upstream of IBV E are expressed in IBV-infected cells (19). The protein encoded by open reading frame 3a is extremely hydrophobic and is predicted to be a membrane protein. It remains possible that the proteins encoded by open reading frames 3a and/or 3b are involved in assembly and budding-site selection, and perhaps they function in concert with the IBV E protein in these processes. We are currently investigating this possibility.

**Possible additional functions of IBV E.** The IBV E protein is abundant in IBV-infected cells at late times postinfection (Fig. 1B), and most or all of the overexpressed protein is found in the Golgi complex (Fig. 7). However, the IBV E protein is only a minor component of virions (20). Thus, some of the cellular E protein might be excluded from assembling virions. It will be interesting to quantitate the IBV E protein in cells and in virions. The high level of E expression in infected cells suggests that it might have additional functions besides its potential role in virus assembly. One possibility is that it induces apoptosis in infected cells, as reported for the MHV E protein (2).

An interesting example of a small membrane protein with potentially more than one function is found in the influenza virus $M_2$ protein, which has some similarities to the coronavirus E protein. It is also a type III integral membrane protein found in much lower levels in virions than in infected cells (16, 41, 43). The function of $M_2$ as a tetrameric ion channel is well characterized (28), but it has also been implicated in assembly. Viruses resistant to plaque growth inhibition induced by a monoclonal antibody to the $M_2$ protein were shown to have compensating mutations in the $M_1$ matrix protein, suggesting that critical interactions between these two proteins occur during budding at the plasma membrane (42). It will be important to address the possible functions of the IBV E protein in infected cells in addition to its potential role in virus assembly.

## ACKNOWLEDGMENTS

We thank M. Delannoy for confocal microscopy expertise and C. Buck for the pSCIIMCS1 vector and helpful advice regarding coinfection with recombinant vaccinia viruses.

This work was supported by National Institutes of Health grant GM42522.

## REFERENCES

1. **Abraham, S., T. E. Kienzle, W. E. Lapps, and D. A. Brian.** 1990. Sequence and expression analysis of potential nonstructural proteins of 4.9, 4.8, 12.7, and 9.5 kDa encoded between the spike and membrane protein genes of the bovine coronavirus. Virology **177:**488–495.
2. **An, S., C. J. Chen, J. L. Leibowitz, and S. Makino.** 1999. Induction of apoptosis in murine coronavirus-infected cultured cells and demonstration of E protein as an apoptosis inducer. J. Virol. **73:**7853–7859.
3. **Baudoux, P., C. Carrat, L. Besnardeau, B. Charley, and H. Laude.** 1998. Coronavirus pseudoparticles formed with recombinant M and E proteins induce alpha interferon synthesis by leukocytes. J. Virol. **72:**8636–8643.
4. **Bos, E. C. W., W. Luytjes, H. Van der Meulen, H. K. Koerten, and W. J. M. Spaan.** 1996. The production of recombinant infectious DI-particles of a

murine coronavirus in the absence of helper virus. Virology **218:**52–60.
5. **Bock, J. B., J. Klumperman, S. Davanger, and R. H. Scheller.** 1997. Syntaxin 6 functions in trans-Golgi network vesicle trafficking. Mol. Biol. Cell **8:**1261–1271.
6. **de Groot, R. J., R. W. van Leen, M. J. M. Dalderup, H. Vennema, M. C. Horzinek, and W. J. M. Spaan.** 1989. Stably expressed FIPV peplomer protein induces cell fusion and elicits neutralizing antibodies in mice. Virology **171:**493–502.
7. **Fischer, F., C. F. Stegen, P. S. Masters, and W. A. Samsonoff.** 1998. Analysis of constructed E gene mutants of mouse hepatitis virus confirms a pivotal role for E protein in coronavirus assembly. J. Virol. **72:**7885–7894.
8. **Fuerst, T. R., E. G. Niles, F. W. Studier, and B. Moss.** 1986. Eukaryotic transient expression system based on recombinant vaccinia virus that synthesizes bacteriophage T7 RNA polymerase. Proc. Natl. Acad. Sci. USA **83:**8122–8126.
9. **Godet, M., R. l'Haridon, J.-F. Vautherot, and H. Laude.** 1992. TGEV coronavirus ORF4 encodes a membrane protein that is incorporated into virions. Virology **188:**666–675.
10. **Hammond, S. A., R. P. Johnson, S. A. Kalams, B. D. Walker, M. Takiguchi, J. T. Safrit, R. A. Koup, and R. F. Siliciano.** 1995. An epitope-selective, transporter associated with antigen presentation (TAP)-1/2-independent pathway and a more general TAP-1/2-dependent antigen-processing pathway allow recognition of the HIV-1 envelope glycoprotein by $CD8^+$ CTL. J. Immunol. **154:**6140–6156.
11. **Holmes, K. V., E. W. Doller, and L. S. Sturman.** 1981. Tunicamycin resistant glycosylation of a coronavirus glycoprotein: demonstration of a novel type of viral glycoprotein. Virology **115:**334–344.
12. **Kim, K. H., K. Narayanan, and S. Makino.** 1997. Assembled coronavirus from complementation of two defective interfering RNAs. J. Virol. **71:**3922–3931.
13. **Klumperman, J., J. Krijnse Locker, A. Meijer, M. C. Horzinek, H. J. Geuze, and P. J. M. Rottier.** 1994. Coronavirus M proteins accumulate in the Golgi complex beyond the site of virion budding. J. Virol. **68:**6523–6534.
14. **Krijnse Locker, J., G. Griffiths, M. C. Horzinek, and P. J. M. Rottier.** 1992. O-glycosylation of the coronavirus M protein. J. Biol. Chem. **267:**14094–14101.
15. **Krijnse Locker, J., M. Ericsson, P. J. M. Rottier, and G. Griffiths.** 1994. Characterization of the budding compartment of mouse hepatitis virus: evidence that transport from the RER to the Golgi complex requires only one vesicular transport step. J. Cell Biol. **124:**55–70.
16. **Lamb, R. A., S. L. Zebedee, and C. D. Richardson.** 1985. Influenza virus $M_2$ protein is an integral membrane protein expressed on the infected-cell surface. Cell **40:**627–633.
17. **Lanser, J., and C. R. Howard.** 1980. The polypeptides of infectious bronchitis virus (IBV-41 Strain). J. Gen. Virol. **46:**349–361.
18. **Lefrancois, L., and D. S. Lyles.** 1982. The interaction of antibody with the major surface glycoprotein of vesicular stomatitis virus. Virology **121:**168–174.
19. **Liu, D. X., D. Cavanagh, P. Green, and S. C. Inglis.** 1991. A polycistronic mRNA specified by the coronavirus infectious bronchitis virus. Virology **184:**531–544.
20. **Liu, D. X., and S. C. Inglis.** 1991. Association of the infectious bronchitis virus 3c protein with the virion envelope. Virology **185:**911–917.
21. **Liu, D. X., and S. C. Inglis.** 1992. Internal entry of ribosomes on a tricistronic mRNA encoded by infectious bronchitis virus. J. Virol. **66:**6143–6154.
22. **Machamer, C. E., and J. K. Rose.** 1987. A specific transmembrane domain of a coronavirus EI glycoprotein is required for its retention in the Golgi region. J. Cell Biol. **105:**1205–1214.
23. **Machamer, C. E., S. A. Mentone, J. K. Rose, and M. G. Farquhar.** 1990. The E1 glycoprotein of an avian coronavirus is targeted to the cis Golgi complex. Proc. Natl. Acad. Sci. USA **87:**6944–6948.
24. **Machamer, C. E., M. G. Grim, A. Esquela, S. W. Chung, M. Rolls, K. Ryan, and A. M. Swift.** 1993. Retention of a *cis* Golgi protein requires polar residues on one face on a predicted a-helix in the transmembrane domain. Mol. Biol. Cell **4:**695–704.
25. **Maeda, J., A. Maeda, and S. Makino.** 1999. Release of coronavirus E protein in membrane vesicles from virus-infected cells and E protein-expressing cells. Virology **263:**265–272.
26. **Nakamura, N., C. Rabouille, R. Watson, T. Nilsson, N. Hui, P. Slusarewicz, T. E. Kries, and G. Warren.** 1995. Characterization of a cis-Golgi matrix protein, GM130. J. Cell Biol. **131:**1715–1726.
27. **Nilsson, I. M., and G. von Heijne.** 1993. Determination of the distance between the oligosaccharyltransferase active site and the endoplasmic reticulum membrane. J. Biol. Chem. **268:**5768–5801.
28. **Pinto, L. H., L. J. Holsinger, and R. A. Lamb.** 1992. Influenza virus $M_2$ protein has ion channel activity. Cell **69:**517–528.
29. **Plutner, H., H. W. Davidson, J. Saraste, and W. E. Balch.** 1992. Morphological analysis of protein transport from the ER to the Golgi membranes in digitonin-permeabilized cells: role of the p58 containing compartment. J. Cell Biol. **119:**1097–1116.
30. **Smith, A. R., M. E. G. Boursnell, M. M. Binns, T. D. K. Brown, and S. C. Inglis.** 1990. Identification of a new membrane-associated polypeptide specified by the coronavirus infectious bronchitis virus. J. Gen. Virol. **71:**3–11.
31. **Stern, D. F., and B. M. Sefton.** 1982. Coronavirus proteins: structure and function of the oligosaccharides of the avian infectious bronchitis virus. J. Virol. **44:**804–812.
32. **Sturman, L. S., K. V. Holmes, and J. Behnke.** 1980. Isolation of coronavirus envelope glycoproteins and interaction with the viral nucleocapsid. J. Virol. **33:**449–462.
33. **Swift, A. M., and C. E. Machamer.** 1991. A Golgi retention signal in a membrane-spanning domain of coronavirus E1 protein. J. Cell Biol. **115:**19–30.
34. **Tooze, J., S. A. Tooze, and S. D. Fuller.** 1987. Sorting of progeny coronavirus from condensed secretory proteins at the exit from the *trans*-Golgi network of AtT20 cells. J. Cell Biol. **105:**1215–1226.
35. **Velasco, A., L. Hendricks, K. W. Moremen, D. R. Tulsiani, O. Touster, and M. G. Farquhar.** 1993. Cell type-dependent variations in the subcellular distribution of alpha-mannosidase I and II. J. Cell Biol. **122:**39–51.
36. **Vennema, H., L. Heijnen, A. Zijderveld, M. C. Horzinek, and W. J. M. Spaan.** 1990. Intracellular transport of recombinant coronavirus spike proteins: implications for viral assembly. J. Virol. **64:**339–346.
37. **Vennema, H., G.-J. Godeke, J. W. A. Rossen, W. F. Voorhout, M. C. Horzinek, D.-J. E. Opstelten, and P. J. M. Rottier.** 1996. Nucleocapsid-independent assembly of coronavirus-like particles by co-expression of viral envelope protein genes. EMBO J. **15:**2020–2028.
38. **von Heijne, G., and Y. Gavel.** 1988. Topogenic signals in integral membrane proteins. Eur. J. Biochem. **174:**671–678.
39. **Weisz, O. A., and C. E. Machamer.** 1994. Use of recombinant vaccinia virus vectors for cell biology. Methods Cell Biol. **43:**137–159.
40. **Yu, X., W. Bi, S. R. Weiss, and J. L. Leibowitz.** 1994. Mouse hepatitis virus gene 5b protein is a new virion envelope protein. Virology **202:**1018–1023.
41. **Zebedee, S. L., and R. A. Lamb.** 1988. Influenza A virus $M_2$ protein: monoclonal antibody restriction of virus growth and detection of $M_2$ in virions. J. Virol. **62:**2762–2772.
42. **Zebedee, S. L., and R. A. Lamb.** 1989. Growth restriction of influenza A virus by $M_2$ protein antibody is genetically linked to the $M_1$ protein. Proc. Natl. Acad. Sci. USA **86:**1061–1065.
43. **Zebedee, S. L., C. D. Richardson, and R. A. Lamb.** 1985. Characterization of the influenza virus $M_2$ integral membrane protein and expression at the infected-cell surface from cloned cDNA. J. Virol. **56:**502–511.